A model for spiral flows in basal ice and the formation of subglacial flutes based on a Reiner-Rivlin rheology for glacial ice

Christian G. Schoof and Garry K.C. Clarke

Department of Earth and Ocean Sciences, University of British Columbia, 6339 Stores Road, Vancouver, Canada, V6T 1Z4

Abstract. Flutes are elongated sediment ridges formed at the base of glaciers and ice sheets. In this paper, we show that flutes can be the product of a corkscrew-like spiral flow in basal ice that removes sediment from troughs between flutes and deposits it at their crests, as first suggested by Shaw and Freschauf. In order to generate the type of basal ice flow required for this mechanism, the viscous rheology of ice must allow for the generation of deviatoric normal stresses transverse to the main flow direction. This type of behavior, which is commonly observed in real nonlinearly viscous and viscoelastic fluids, can be described by a Reiner-Rivlin rheology. Here, we develop a mathematical model that describes the role of these transverse stresses in generating spiral flows in basal ice, and investigate how these flows lead to the amplification of initially small basal topography and the eventual formation of assemblies of evenly spaced subglacial flutes.

1. Introduction

Subglacial flutes are ubiquitous features of deglaciated landscapes, both modern and ancient. Their shape is that of a highly elongated ridge aligned with the former direction of ice flow, which indicates a subglacial origin. Flutes, like other streamlined glacial bedforms such as drumlins, tend to occur in large groups with many individual ridges of similar dimensions aligned in the same direction (figure 1). Flutes can range in size from the relatively small ridges commonly found on the forefields of retreating valley glaciers, with individual flute widths and heights on the order of decimeters to metres [e.g. *Boulton*, 1976; *Ottesen and Dowdeswell*, 2006] and lengths of a hundred or so meters up to a kilometre, to the vast 'megaflutes' formed by the Laurentide ice sheet [e.g. *Smith*, 1948; *Shaw and Freschauf*, 1973] and the Antarctic ice sheet [*Dowdeswell et al.*, 2004; *Mosola and Anderson*, 2006; *Ó Cofaigh et al.*, 2005], where individual ridges can be tens of meters tall, around a hundred meters wide, and many tens of kilometers long.

Given the obvious disparity in size, megaflutes (also known as mega-scale glacial lineations) may be formed differently from their smaller-scale counterparts under valley glaciers, but in the absence of a conclusive formation mechanism, this remains conjecture. Flutes, or at least megaflutes, are believed to be the end-member of a spectrum of streamlined subglacial bedforms, which also includes less elongated ridges known as drumlins and ridges transverse to ice flow known as Rogen moraine [*Lundqvist*, 1969; *Glückert*, 1973; *Aario*, 1977]. The mechanism by which streamlined subglacial bedforms are formed is not known. Various theories for bedform genesis have been proposed [*Tarr*, 1894; *Gravenor*, 1953; *Smalley and Unwin*, 1968; *Shaw*, 1983; *Boulton*, 1987; *Menzies and Rose*, 1987], but few have been tested using physics-based quantitative models [*Morris and Morland*, 1976; *Hindmarsh*, 1998; *Fowler*, 2000, 2001; *Clark et al.*, 2003; *Schoof*, 2002, 2007a, b]. *Hindmarsh* [1998] and *Fowler* [2000, 2001] advanced the concept that subglacial bedforms are the result of an instability in the transport of subglacial sediment. Specifically, they assume that a positive feedback mechanism between the presence of subglacial topography, perturbations in basal ice flow and sediment transport leads to the amplification of subglacial topography, and that this amplification favours certain wavelengths (this being a generic feature of continuum mechanical instabilities). This type of formation mechanism would therefore account for the emergence of a dominant wavelength in subglacial topography, and would explain the quasi-regular pattern of typical drumlin, Rogen moraine and flute fields.

By contrast, the theories of *Boulton* [1976], *Morris and Morland* [1976] and *Clark et al.* [2003] do not involve an instability but require the presence of pre-existing protuberances on the glacier or ice sheet bed. These protuberances effectively force the formation of sediment ridges in their lee. While this kind of 'forced' mechanism can undoubtedly explain the formation of some bedforms, it is less appealing as an explanation than an instability because it requires a regularly sized and spaced protuberances in order to account for the the formation of large fields of drumlins or flutes [or indeed smaller glacial flutes, see the flute spacing histograms om figure 17 of *Boulton*, 1976]. There is evidence that smaller flutes exposed in the forefield of valley glaciers often have a boulder embedded in till at their upstream end. This does point to protuberances playing an important role at least in determining the location of bedforms, but is not by itself evidence against an instability mechanism: if there are protuberances on the bed, these will naturally act as 'seeds' for the instability [see also *Rose*, 1989]. We will return to a brief discussion of Boulton's theory, which is built on the association between small flutes and boulders, in section 4.

In the main part of this paper, we investigate a new instability mechanism that differs in the physics involved from the mechanism proposed by *Hindmarsh* [1998] and *Fowler* [2000, 2001] and investigated by *Schoof* [2007a, b], but could explain some conjectures made in the past in the geomorphological literature. Based on an idea due to *Shaw and Freschauf* [1973] the mechanism we study here envisions the formation of secondary, transverse flows in basal ice that remove sediment from the troughs between bedforms and deposit it at the crest (see figure 1). Shaw and Freschauf proposed this mechanism on the basis of herringbone-type fabric patterns in megaflutes that are indicative of sediment having been moved from inter-flute troughs to flute crests [see also *Rose*, 1989].

In fluvial bedform formation, a transverse component of sediment transport could arise due to secondary flows in

0148-0227/07/$9.00

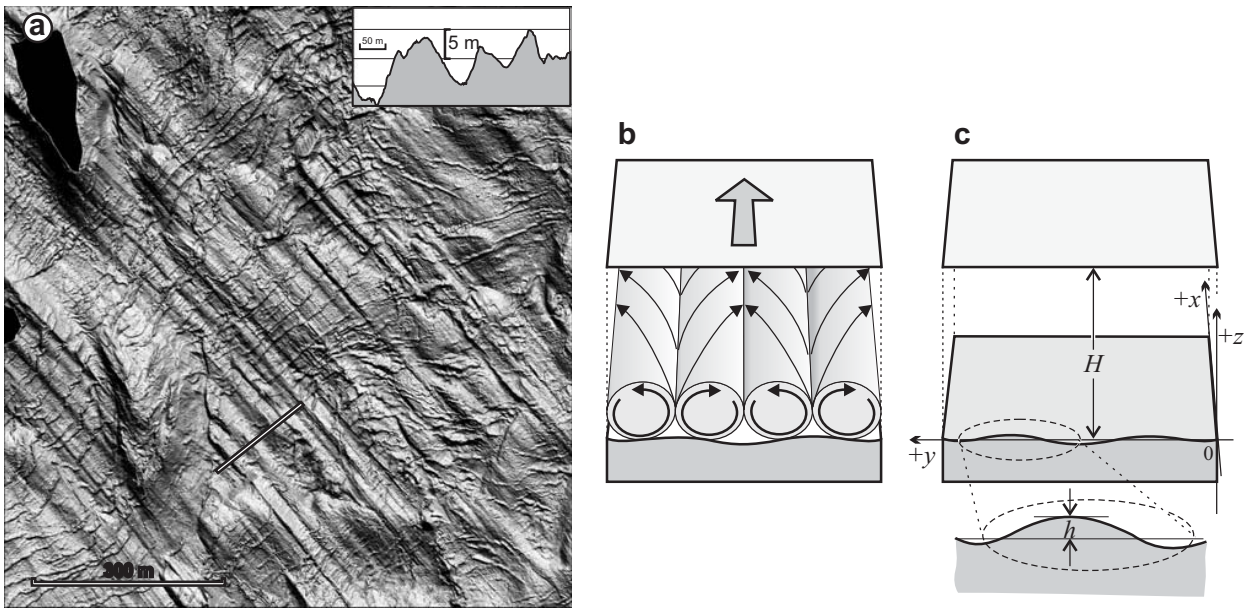

Figure 1. Panel a shows a swath-bathymetric relief image of subglacial bedforms in Borebukta, Svalbard, in which subglacial flutes (oriented bottom right to top left) are clearly visible. Reproduced from *Ottesen and Dowdeswell* [2006], copyright American Geophysical Union (2006). Panel b illustrates the formation of spiral flows in basal ice, removing sediment from flute troughs and depositing it on flute crests. Panel c shows the geometry used in our model.

the turbulent motion of water and sediment entrainment into the flow itself. Neither of these physical ingredients — turbulence or entrainment of sediment into the flow — is relevant to the flow of ice. In fact, the generation of secondary, transverse flows in ice is not straightforward: if the rheology of ice (assumed incompressible) is such that strain rate and deviatoric stress are parallel [i.e., related to each other by a scalar viscosity, as for instance in Glen's law, see *Paterson*, 1994, chapter 5], and if there are no bed undulations or variations in basal friction along the flow direction, then no transverse flow will occur [this flow geometry then gives rise to the unidirectional flow solutions found in e.g. *Nye*, 1965; *Reynaud*, 1973; *Truffer and Echelmeyer*, 2003; *Schoof*, 2006a].

An alternative way of generating secondary flows is therefore required. The mechanism we explore here assumes that deviatoric stress τ_{ij} and strain rate D_{ij} are not parallel, but related through a more general Reiner-Rivlin rheology [e.g. *Eringen*, 1962]:

$$\tau_{ij} = 2\eta D_{ij} + 4\mu \left(D_{ik}D_{kj} - \frac{1}{3} D_{kl}D_{kl}\delta_{ij} \right). \qquad (1)$$

Here, ice is assumed to be incompressible ($D_{ii} = 0$) and strain rate is related to the velocity field $\mathbf{u}$ in the usual way through

$$D_{ij} = \frac{1}{2} \left(\frac{\partial u_i}{\partial x_j} + \frac{\partial u_j}{\partial x_i} \right). \qquad (2)$$

The first term in (1) is the usual viscous stress term. $\eta > 0$ is the ordinary viscosity and may depend on the invariants of $\mathbf{D}$. The second term in (1) is in general not parallel to D_{ij} and generates so-called normal stress effects. Specifically, this term gives rise to deviatoric normal stresses transverse to flow in a simple shearing flow: if the velocity field in a Cartesian $Oxyz$ coordinate system takes the form of a simple shearing (Couette) flow with $\mathbf{u} = (\tau_0 z/\eta, 0, 0)$, then

$$\frac{\boldsymbol{\tau}}{\tau_0} = \begin{pmatrix} 0 & 0 & 1 \\ 0 & 0 & 0 \\ 1 & 0 & 0 \end{pmatrix} + \frac{\mu\tau_0}{\eta^2} \begin{pmatrix} \frac{1}{3} & 0 & 0 \\ 0 & -\frac{2}{3} & 0 \\ 0 & 0 & \frac{1}{3} \end{pmatrix}. \qquad (3)$$

Clearly, the second matrix represents normal stresses generated by the shearing flow, and these scale to the basic shear stress τ_0 as $\mu\tau_0/\eta^2$. The importance of the second term to the stress field is therefore small when $\mu\tau_0/\eta^2$ is much less than one. We will make use of this approximation in the later stages of the analysis in this paper to gain insight into qualitative aspects of normal stress effects, but as we will see in section 4, experimental evidence suggests that normal stress effects may in fact be comparable to classical viscous effects on stress in some glacial settings: the contribution of the second term in (1) may be comparable to the contribution of the first term.

The role played by transverse normal stresses in generating secondary, transverse flows is relatively simple to understand: if the main shearing flow, say in the x-direction, is not uniform, then the normal stresses which this main flow generates in the yz-plane are themselves not uniform. In order to balance these stresses, additional stresses are required in the yz-plane, and these must be supplied by a secondary, transverse flow [*Eringen*, 1962]. Just as importantly, deviatoric stresses transverse to flow at a boundary may have to be counteracted by stresses that can only be supplied by a secondary flow. As we will see below, this type of boundary stress is the main driver for secondary, transverse flows in the glacial setting considered in this paper.

We emphasize that our aim in this paper is conceptual. Although the possibility of normal stress effects was acknowledged in the original paper by *Glen* [1958], almost all theoretical studies of glacier flow have hitherto relied on simpler rheological models in which deviatoric stress τ_{ij} is parallel to strain rate D_{ij}. It is idle to speculate as to the reasons for this, but the additional complexity of including higher-order rheological effects probably accounts for the choice of a simpler rheological model. There is, however,

empirical evidence for non-normal stress effects in the viscous deformation of ice published by *McTigue et al.* [1985] and *Man and Sun* [1987], and reviewed by *van der Veen and Whillans* [1990]. If one uses the rheological model (1), these studies indicate that $\mu > 0$. The effect of such a rheology on glacier flow has not yet been explored in detail, but current evidence shows that only small differences would be expected in large-scale ice flow from the predictions of a model with $\mu = 0$: principally, one would expect a slight deformation in the upper surface of mountain glaciers [*McTigue et al.*, 1985; *Man and Sun*, 1987], specifically a surface depression in the centre with amplitude on the order of 10 m for a glacier with semicircular cross-section of radies 500 m, and a smaller surface depression for thinner ice [see figure 4 of *McTigue et al.*, 1985]. It is worth pointing out, however, that the potential effect of normal stress effects on isochrone layers in ice sheets [e.g. *Parrenin and Hindmarsh*, 2007] has not yet been studied; if our theory is correct, then one may expect to see significant disturbances in isochrone layers in basal ice, including complete overturning, and this is is a possible avenue for testing the proposed theory against non-geomorphological field data.

In the remainder of this paper, we focus solely on the possibility that normal stress effects could have significant effect on ice flow near the bed, and account for the formation of subglacial bedforms. In particular, we investigate whether small undulations in the bed in conjunction with normal stress effects in the ice could cause the formation of secondary flows and the subsequent amplification of the bed undulations. Our focus in this papers is on flutes — bedforms whose cross-section is uniform in the main ice flow direction — mainly as a matter of convenience as it allows us to deal with a simpler, two-dimensional mathematical model, but it is possible that an analogous three-dimensional model could also explain three-dimensional bedforms such as drumlins.

2. The model

We consider a flow geometry in which the mean flow direction is aligned with the x-axis, and only allow bed elevation to depend on the transverse y-coordinate. Specifically, we let the ice-bed interface be at $z = h(y)$, where z is measured vertically upwards (in terms of geomorphology, this implies that we are not able to consider more complicated, three-dimensional basal topography such as drumlins, but will only study flutes). Unit vectors in the x-, y- and z-directions will be denoted by $\mathbf{i}$, $\mathbf{j}$ and $\mathbf{k}$, respectively. To clarify the use of subscripts in tensor notation, we put $(x, y, z) = (x_1, x_2, x_3)$. Similarly, we assume that the velocity field $\mathbf{u} = (u, v, w) = (u_1, u_2, u_3)$ depends only on y and z. Then the strain rate tensor can be written in matrix form as

$$\mathbf{D} = \begin{pmatrix} 0 & \frac{1}{2}\frac{\partial u}{\partial y} & \frac{1}{2}\frac{\partial u}{\partial z} \\ \frac{1}{2}\frac{\partial u}{\partial y} & \frac{\partial v}{\partial y} & \frac{1}{2}\left(\frac{\partial v}{\partial z} + \frac{\partial w}{\partial y}\right) \\ \frac{1}{2}\frac{\partial u}{\partial z} & \frac{1}{2}\left(\frac{\partial v}{\partial z} + \frac{\partial w}{\partial y}\right) & \frac{\partial w}{\partial z} \end{pmatrix}. \quad (4)$$

We also extend the flow domain to $z = \infty$, and apply far-field boundary conditions representing hydrostatic normal stress and uniform shear stress far above the bed.

On $h < z < \infty$, we have the usual Stokes equations

$$\frac{\partial \tau_{ij}}{\partial x_j} - \frac{\partial p}{\partial x_i} - \rho g \delta_{i3} = 0, \quad (5)$$

$$\nabla \cdot \mathbf{u} = \frac{\partial v}{\partial y} + \frac{\partial w}{\partial z} = 0. \quad (6)$$

Here, p is pressure, ρ is the density of ice and g is acceleration due to gravity.

We assume that the bed is a material surface (i.e., we ignore the effect of melting or freezing), and impose the kinematic boundary condition

$$w = v\frac{\partial h}{\partial y} + \frac{\partial h}{\partial t}. \quad (7)$$

Further, we assume that the bed is Coulomb-plastic [*Iverson et al.*, 1998]. Specifically, we assume that basal shear stress $\tilde{\tau}_{(b)i}$ is rate-independent (independent of sliding speed), and its modulus is related to basal water pressure p_w and to compressive normal stress ($-\sigma_{nn} = p - \tau_{ij}n_in_j$ in the usual notation) through

$$\tilde{\tau}_{(b)} = \nu(-\sigma_{nn} - p_w). \quad (8)$$

ν is the basal friction coefficient, not to be confused with the viscosity coefficient μ. In the sequel, we take p_w to be a constant prescribed by a drainage system, which we do not model explicitly.

It remains to specify a direction for the basal shear stress. Naturally, friction has to resist motion, and if the bed is isotropic we expect basal shear stress to be parallel to the direction of basal velocity. There is a small complication: velocity $\mathbf{u}$ at the bed may have a component normal to the bed if the bed evolves in time, while the shear stress vector $\tilde{\boldsymbol{\tau}}_{(b)}$ must be parallel to the bed. Hence we take the direction of $\tilde{\boldsymbol{\tau}}_{(b)}$ to be that of the projection of velocity onto the bed, i.e., $\mathbf{u} - (\mathbf{u}\cdot\mathbf{n})\mathbf{n}$, so

$$\tilde{\tau}_{(b)i} = \nu(-\sigma_{nn} - p_w)\frac{u_i - u_jn_jn_i}{|\mathbf{u} - (\mathbf{u}\cdot\mathbf{n})\mathbf{n}|}. \quad (9)$$

Here, $\mathbf{n}$ is the unit normal to the bed,

$$\mathbf{n} = \frac{\left(0, -\frac{\partial h}{\partial y}, 1\right)}{\sqrt{1 + \left(\frac{\partial h}{\partial y}\right)^2}}. \quad (10)$$

Of course, we have to assume that the tangential component of velocity at the bed is non-zero, i.e., that the ice is sliding, as otherwise the tangential velocity vector $\mathbf{u} - (\mathbf{u}\cdot\mathbf{n})\mathbf{n}$ does not have a direction associated with it.

In terms of deviatoric stress τ_{ij} and pressure p, we obtain the relation

$$\begin{aligned} \tilde{\tau}_{(b)i} &= \tau_{jk}(\delta_{ij}n_k - n_in_jn_k) \\ &= \nu(p - \tau_{jk}n_jn_k - p_w)\frac{u_i - u_ln_ln_i}{|\mathbf{u} - (\mathbf{u}\cdot\mathbf{n})\mathbf{n}|}, \end{aligned} \quad (11)$$

where $\tau_{jk}(\delta_{ij}n_k - n_in_jn_k)$ is the basal shear stress, defined simply as the tangential component of the deviatoric part of interfacial traction, $\tau_{ij}n_j$. (To get the tangential component, we simply subtract the normal component, $n_i \times \tau_{jk}n_jn_k$.)

We still have to model the evolution of the bed as driven by the flow of ice. The simplest way to model the ice flow–sediment transport interactions involved is to suppose that till flux is proportional to ice velocity at the ice-till interface, which we adopt here. This may be contrasted with descriptions of till flux in models for subglacial bedform formation [e.g. *Hindmarsh*, 1998; *Fowler*, 2000; *Schoof*, 2007a], which additionally require a dependence of till flux on effective pressure. A plausible basis for our till flux assumption

is the following. Suppose that a constant thickness of sediment, determined by the size of clasts embedded in basal ice, is moved with the ice by ploughing, and suppose that this till layer moves at a constant fraction of the basal ice velocity. The horizontal component of sediment flux is then simply

$$\mathbf{q}_s = d_s(u\mathbf{i} + v\mathbf{j})|_{z=h}, \tag{12}$$

where d_s is a constant of proportionality with dimensions of length. Roughly speaking, d_s is the depth to which the till is ploughed. We acknowledge at this point that our description of sediment transport is somewhat simplistic and cannot account for deformation at significant depth in the underlying till, which could conceivably be described by a viscous model for till [e.g. *Boulton and Hindmarsh*, 1987]. In fact, for a till with constant viscosity, (12) would still hold approximately (at least for the sediment flowing in simple shear) with d_s equal to the thickness of the till layer. The sliding law (11) is the main model component that would need to be altered for a viscous till description. Although we do not go into detail here, a viscous model for sliding and till deformation would not substantially alter our main result, namely that a general Reiner-Rivlin rheology can lead to secondary, transverse flows in basal ice and the amplification of sediment rides at the bed, as this is predicated only on the occurrence of normal stress effects in the ice and not on the particulars of the sediment flow rule. As we will see in section 4, sediment transport does affect some other aspects of the flute-forming process, but we defer a consideration of those to future work.

Proceeding with (12) and noting that u is independent of x, the bed then evolves according to the sediment conservation equation

$$\frac{\partial h}{\partial t} + d_s \frac{\partial v|_{z=h}}{\partial y} = 0. \tag{13}$$

Lastly, we require a hydrostatic normal stress and a uniform shear stress τ_b in the far field ($z \to \infty$), while velocity approaches a simple shearing profile:

$$p - \tau_{33} \sim \rho g(H - z), \qquad \tau_{13} \sim \tau_b,$$

$$\tau_{23} \sim 0, \qquad u \sim u_b + \tau_b z/\eta. \tag{14}$$

Here H is the thickness of overlying ice, assumed to be large compared with the length scale relevant to basal topography. In this context, $z \to \infty$ is to be interpreted in the sense of boundary layer theory as being z much larger than the basal topography length scale (the inner scale relevant to ice flow near the bed) but small compared with overall ice thickness (the outer scale germane to the large-scale flow of the ice mass). τ_b is the basal shear stress experienced by the large-scale flow of the ice sheet, smoothed over small-scale basal variations [see also *Fowler*, 1981], and the expressions for $p - \tau_{33}$, τ_{13} and τ_{23} are chosen to force stresses in the basal boundary layer to approach the stress field expected in the bulk of the ice flow at long distances from the bed. With a Coulomb friction law, this smoothed shear stress cannot be imposed arbitrarily, but must be determined through an average of the yield stress at the bed. Conversely, the flow problem considered here will not provide a value of the mean sliding velocity u_b, and a solution of the large scale flow of the ice sheet as described in *Schoof* [2006b] is then required to provide this velocity u_b [see also *Schoof*, 2007a, section 7]. Here, we do not solve such a large-scale model — our interest is purely in small-scale flow features near the bed — and simply take u_b as given. The first part of the next section will clarify these points.

3. Stability analysis

3.1. The basic state: laminar flow

We begin with the solution for a flat bed as the basic state which is then perturbed slightly. The basic objective of a linear stability analysis is to determine if these slight perturbations continue to grow, i.e., to see if the flat bed is unstable to the amplification of small bed topography, and to determine which wavelengths grow fastest. For simplicity, we assume that the viscosities η and μ are constant.[1]

The basic solution for a flat bed $h \equiv 0$ is

$$u = u_b + \tau_b z/\eta, \qquad v = w = 0. \tag{15}$$

As noted at the end of the last section, τ_b must in fact be determined by basal conditions, and we must have from (11) that

$$\tau_b = \nu(p - \tau_{33} - p_w). \tag{16}$$

But by the z-component of the Stokes equations (5), combined with the far-field conditions (14), we have the 'hydrostatic' prescription for stress,

$$p - \tau_{33} = \rho g H, \tag{17}$$

and hence the simple relationship

$$\tau_b = \nu(\rho g H - p_w). \tag{18}$$

Moreover, we can compute $\tau_{33} = \mu\tau_b^2/(3\eta^2)$ (see also equation (3)), and so

$$p = \rho g H + \frac{\mu\tau_b^2}{3\eta^2}. \tag{19}$$

There is however nothing to fix the basal velocity u_b in (15). As discussed at the end of the previous section, because Coulomb friction is not rate-limiting, this sliding velocity must in fact be supplied by the large-scale flow of the ice sheet over a Coulomb-plastic bed, as described in detail in *Schoof* [2004, 2006b]. Here we simply assume that its value is known.

3.2. Perturbations to the basic state

Our next step is to introduce a small perturbation $h(y)$ of amplitude comparable to some small value δ into the bed, which causes a small perturbation in the velocity and stress fields. We let $\mathbf{u} = \mathbf{u}^{(0)} + \delta\mathbf{u}^{(1)} + O(\delta^2)$, $p = p^{(0)} + \delta p^{(1)} + O(\delta^2)$, with $\mathbf{u}^{(0)}$ and $p^{(0)}$ given by (15) and (19), and put $\mathbf{D} = \mathbf{D}^{(0)} + \delta\mathbf{D}^{(1)}$, $h = \delta h^{(1)} + O(\delta^2)$. Then

$$\mathbf{D}^{(0)} = \begin{pmatrix} 0 & 0 & \frac{\tau_b}{2\eta} \\ 0 & 0 & 0 \\ \frac{\tau_b}{2\eta} & 0 & 0 \end{pmatrix}, \tag{20}$$

$$\mathbf{D}^{(1)} = \begin{pmatrix} 0 & \frac{1}{2}\frac{\partial u^{(1)}}{\partial y} & \frac{1}{2}\frac{\partial u^{(0)}}{\partial z} \\ \frac{1}{2}\frac{\partial u^{(1)}}{\partial y} & \frac{\partial v^{(1)}}{\partial y} & \frac{1}{2}\left(\frac{\partial v^{(1)}}{\partial z} + \frac{\partial w^{(1)}}{\partial y}\right) \\ \frac{1}{2}\frac{\partial u^{(1)}}{\partial z} & \frac{1}{2}\left(\frac{\partial v^{(1)}}{\partial z} + \frac{\partial w^{(1)}}{\partial y}\right) & \frac{\partial w^{(1)}}{\partial z} \end{pmatrix}. \tag{21}$$

Continuing in the same notation, we have

$$\boldsymbol{\tau}^{(0)} = \tau_b \begin{pmatrix} 0 & 0 & 1 \\ 0 & 0 & 0 \\ 1 & 0 & 0 \end{pmatrix} + \frac{\mu\tau_b^2}{\eta^2} \begin{pmatrix} \frac{1}{3} & 0 & 0 \\ 0 & -\frac{2}{3} & 0 \\ 0 & 0 & \frac{1}{3} \end{pmatrix}. \tag{22}$$

$$\tau_{ij}^{(1)} = 2\eta D_{ij}^{(1)} + 4\mu\left(D_{ik}^{(0)}D_{kj}^{(1)} + D_{ik}^{(1)}D_{kj}^{(0)} - \frac{2}{3}D_{kl}^{(1)}D_{kl}^{(0)}\delta_{ij}\right), \quad (23)$$

so

$$\boldsymbol{\tau}^{(1)} = 2\eta\mathbf{D}^{(1)} + \frac{2\tau_b\mu}{\eta}\begin{pmatrix} \frac{2}{3}D_{13}^{(1)} & D_{23}^{(1)} & D_{33}^{(1)} \\ D_{23}^{(1)} & -\frac{4}{3}D_{13}^{(1)} & D_{12}^{(1)} \\ D_{33}^{(1)} & D_{12}^{(1)} & \frac{2}{3}D_{13}^{(1)} \end{pmatrix}, \quad (24)$$

omitting quadratic terms in δ.

The Stokes equations at $O(\delta)$ are

$$\frac{\partial\tau_{ij}^{(1)}}{\partial x_j} - \frac{\partial p^{(1)}}{\partial x_i} = 0, \quad (25)$$

which combined with (24) and the assumption that p and $\mathbf{u}$ do not depend on x retrieves the equations

$$\frac{\partial v^{(1)}}{\partial y} + \frac{\partial w^{(1)}}{\partial z} = 0, \quad (26)$$

$$\eta\left(\frac{\partial^2}{\partial y^2} + \frac{\partial^2}{\partial z^2}\right)u^{(1)} + \frac{2\tau_b\mu}{\eta}\left(\frac{\partial^2 w^{(1)}}{\partial z^2} + \frac{1}{2}\frac{\partial^2 w^{(1)}}{\partial y^2} + \frac{1}{2}\frac{\partial^2 v^{(1)}}{\partial y\partial z}\right) = 0, \quad (27)$$

$$\eta\left(\frac{\partial^2}{\partial y^2} + \frac{\partial^2}{\partial z^2}\right)v^{(1)} - \frac{\partial p^{(1)}}{\partial y} - \frac{2\tau_b\mu}{3\eta}\frac{\partial^2 u^{(1)}}{\partial y\partial z} = 0, \quad (28)$$

$$\eta\left(\frac{\partial^2}{\partial y^2} + \frac{\partial^2}{\partial z^2}\right)w^{(1)} - \frac{\partial p^{(1)}}{\partial z} + \frac{2\tau_b\mu}{\eta}\left(\frac{1}{3}\frac{\partial^2 u^{(1)}}{\partial z^2} + \frac{1}{2}\frac{\partial^2 u^{(1)}}{\partial y^2}\right) = 0. \quad (29)$$

We also linearize the domain, and thus impose (27)–(26) on $0 < z < \infty$ rather than on $\delta h^{(1)} + O(\delta^2) < z < \infty$.

Boundary conditions at the bed are found by linearizing around the unperturbed position $z = 0$. The kinematic condition (7) simply becomes

$$w^{(1)} = \frac{\partial h^{(1)}}{\partial t}, \quad (30)$$

again omitting terms of $O(\delta^2)$.

Equation (30) contains the rate of bed change, which the sediment continuity equation (13) specifies in terms of $v^{(1)}$:

$$\frac{\partial h^{(1)}}{\partial t} + d_s\frac{\partial v^{(1)}|_{z=0}}{\partial y} = 0. \quad (31)$$

Further coupling of the flow with the small bed perturbations arises through friction at the bed. We therefore need to consider the first-order correction to basal friction, and this involves a certain amount of work which takes up the remainder of this section. In essence, what we find is that the magnitude of basal shear stress remains unaltered at first order, but that its direction is altered by the presence of a transverse component of flow. We put

$$\mathbf{n}^{(0)} = (0,0,1), \qquad \mathbf{n}^{(1)} = \left(0, -\frac{\partial h^{(1)}}{\partial y}, 0\right). \quad (32)$$

Further, at the bed $z = h$, velocity $\mathbf{u}$ can be written to order $O(\delta)$ as

$$\mathbf{u} = \mathbf{u}^{(0)}|_{z=0} + \delta(\tau_b h^{(1)}/\eta + \mathbf{u}^{(1)}), \quad (33)$$

where the first term in brackets arises from Taylor expanding about $z = 0$ to find velocity at $z = \delta h^{(1)} + O(\delta^2)$. Since $\mathbf{u}^{(0)}\cdot\mathbf{n}^{(0)} = \mathbf{u}^{(0)}\cdot\mathbf{n}^{(1)} = 0$ and $\mathbf{u}^{(1)}\cdot\mathbf{n}^{(0)} = w^{(1)}$,

$$\mathbf{u} - (\mathbf{u}\cdot\mathbf{n})\mathbf{n} = \left[u_b + \delta(\tau_b h^{(1)}/\eta + u^{(1)})\right]\mathbf{i} + \delta v^{(1)}\mathbf{j} + O(\delta^2), \quad (34)$$

$$|\mathbf{u} - (\mathbf{u}\cdot\mathbf{n})\mathbf{n}| = u_b + \delta(\tau_b h^{(1)}/\eta + u^{(1)}) + O(\delta^2). \quad (35)$$

Combining these results, the along-flow tangent vector can be shown to be

$$\frac{\mathbf{u} - (\mathbf{u}\cdot\mathbf{n})\mathbf{n}}{|\mathbf{u} - (\mathbf{u}\cdot\mathbf{n})\mathbf{n}|} = \mathbf{i} + \frac{\delta v^{(1)}}{u_b}\mathbf{j} + O(\delta^2). \quad (36)$$

We linearize the left-hand side of (11) as

$$\tilde{\tau}_{(b)i}^{(1)} = \tau_{jk}^{(1)}\left(\delta_{ij}n_k^{(0)} - n_i^{(0)}n_j^{(0)}n_k^{(0)}\right) + \tau_{jk}^{(0)}\Big(\delta_{ij}n_k^{(1)} - n_i^{(1)}n_j^{(0)}n_k^{(0)} - n_i^{(0)}n_j^{(1)}n_k^{(0)} - n_i^{(0)}n_j^{(0)}n_k^{(1)}\Big), \quad (37)$$

where all quantities are evaluated at $z = 0$. (Because the unperturbed shear stress $\tau_{13}^{(0)}$ is independent of z, no term arises at $O(\delta)$ from Taylor expanding about $z = 0$.) Making the appropriate substitutions, we find

$$\tilde{\boldsymbol{\tau}}_{(b)}^{(1)} = \begin{pmatrix} \tau_{13}^{(1)} \\ \tau_{23}^{(1)} \\ 0 \end{pmatrix} - \frac{\partial h^{(1)}}{\partial y}\begin{pmatrix} \tau_{12}^{(0)} \\ \tau_{22}^{(0)} - \tau_{33}^{(0)} \\ -\tau_{23}^{(0)} \end{pmatrix} = \eta\begin{pmatrix} \frac{\partial u^{(1)}}{\partial z} \\ \frac{\partial v^{(1)}}{\partial z} + \frac{\partial w^{(1)}}{\partial y} \\ 0 \end{pmatrix} + \frac{\tau_b\mu}{\eta}\begin{pmatrix} 2\frac{\partial w^{(1)}}{\partial z} \\ \frac{\partial u^{(1)}}{\partial y} \\ 0 \end{pmatrix} + \frac{\tau_b^2\mu}{\eta^2}\frac{\partial h^{(1)}}{\partial y}\begin{pmatrix} 0 \\ 1 \\ 0 \end{pmatrix}. \quad (38)$$

Similarly, we linearize the term $\nu(p - \tau_{kl}n_k n_l - p_w)$ on the right-hand side of (11) to find the $O(\delta)$ correction

$$\nu\left(p^{(1)} - \rho g h^{(1)} - \tau_{kl}^{(1)}n_k^{(0)}n_l^{(0)} - \tau_{kl}^{(0)}n_k^{(1)}n_l^{(0)} - \tau_{kl}^{(0)}n_k^{(0)}n_l^{(1)}\right)$$

$$= \nu\left(p^{(1)} - \rho g h^{(1)} - \tau_{33}^{(1)} + 2\frac{\partial h^{(1)}}{\partial y}\tau_{23}^{(0)}\right) = \nu\left(p^{(1)} - \rho g h^{(1)} - \tau_{33}^{(1)}\right) = \nu\left(p^{(1)} - \rho g h^{(1)} - 2\eta\frac{\partial w^{(1)}}{\partial z} - \frac{2\tau_b\mu}{3\eta}\frac{\partial u^{(1)}}{\partial z}\right), \quad (39)$$

where again all quantities are evaluated at $z = 0$. The $O(\delta)$ correction for the entire right-hand side of (11) becomes, from (39) and (36):

$$\frac{\tau_b}{u_b}\begin{pmatrix} 0 \\ v^{(1)} \\ 0 \end{pmatrix} + \nu\left(p^{(1)} - \rho g h^{(1)} - 2\eta\frac{\partial w^{(1)}}{\partial z} - \frac{2\tau_b\mu}{3\eta}\frac{\partial u^{(1)}}{\partial z}\right)\begin{pmatrix} 1 \\ 0 \\ 0 \end{pmatrix} \quad (40)$$

Equating the expressions in (38) and (40) finally gives us two more explicit boundary conditions at $z = 0$ in addition

to (30):

$$\eta\frac{\partial u^{(1)}}{\partial z}+2\frac{\tau_b\mu}{\eta}\frac{\partial w^{(1)}}{\partial z} = \nu\left(p^{(1)}-\rho g h^{(1)}-2\eta\frac{\partial w^{(1)}}{\partial z}-\frac{2\tau_b\mu}{3\eta}\frac{\partial u^{(1)}}{\partial z}\right), \quad (41)$$

$$\eta\left(\frac{\partial v^{(1)}}{\partial y}+\frac{\partial w^{(1)}}{\partial y}\right)+\frac{\tau_b\mu}{\eta}\frac{\partial u^{(1)}}{\partial y}+\frac{\partial h^{(1)}}{\partial y}\frac{\tau_b^2\mu}{\eta^2}=\frac{\tau_b v^{(1)}}{u_b} \quad (42)$$

The term in these boundary conditions that will be of central importance later is the term $\tau_b^2\mu/\eta^2\times\partial h^{(1)}/\partial y$ on the left-hand side of (42). This term represents the effect of zeroth-order vertical deviatoric stresses at the bed, which have a small component parallel to the bed in the presence of small bed corrugations, represented here by $\partial h^{(1)}/\partial y$. In the Newtonian case, where $\mu=0$ and the Reiner-Rivlin term in (1) is absent, no such stress effect occurs at the boundary.

Incidentally, the form of (42) is not sensitive to changing the basal friction law: the term $\tau_b^2\mu/\eta^2\times\partial h^{(1)}/\partial y$ which we have identified as critical results from linearizing the expression for basal shear stress rather than the friction law. Instead, the friction law contributes the term $\tau_b v^{(1)}/u_b$ on the right-hand side. An similar analysis with a power-law friction law [e.g. *Weertman*, 1957] results in the same term appearing on the right-hand side. As a consequence, the linear stability analysis presented later is unaltered under a change in the basal friction law, and the instability mechanism is essentially independent of the details of friction at the bed.

Lastly, the far-field boundary conditions (14) give

$$\tau_{13}^{(1)}\sim\tau_{23}^{(1)}\sim p^{(1)}-\tau_{33}^{(1)}\sim 0 \quad (43)$$

as $z\to\infty$.

3.3. Further simplification

Although the modified Stokes flow problem (27)–(26) with (30) and (41)–(43) is linear and amenable to solution by Fourier transforms, this procedure still requires a formidable amount of algebra and the resulting expressions are not simple to interpret. Consequently, we apply a further simplification to the model before we forge ahead with a linear stability analysis.

Our motivation is this: in ice sheet modelling, the second term in (1) is usually ignored (while η is treated as strain-rate dependent through Glen's law). Ignoring the second term in (1) is justified if this term is small, though not necessarily equal to zero — in other words, if μ is sufficiently small. As ice sheets appear to be well-described by models that omit the second term on the right-hand side of (1), we suppose that μ is indeed small, and proceed on that basis.

We have to be careful about precisely what we mean by 'small', and this is understood most easily in terms of stresses. We may consider τ_b/η as a measure of strain rate, and hence typical stresses predicted by the first term in (1) are comparable to τ_b, while those predicted by the second term are of order $\mu\times\tau_b^2/\eta^2$. If these secondary stresses are small, then we must have $\mu\tau_b^2/\eta^2\ll\tau_b$ or

$$\frac{\mu\tau_b}{\eta^2}\ll 1. \quad (44)$$

We assume this to be the case in what follows, and approximate the linearized problem (27)–(26) with (30) and (41)–(43) correspondingly, treating the Reiner-Rivlin viscosity parameter $\mu\tau_b/\eta^2$ as small (realistic values for $\mu\tau_b/\eta^2$ are discussed further in section 4). This could be done formally by scaling the problem and using a perturbation expansion, but the procedure would be unnecessarily cumbersome and yield the same result as the more informal derivation below.

The leading order approximation in $\mu\tau_b/\eta^2$ corresponds to dropping all terms that include a factor μ in (26)–(29), (30) and (41)–(43). We obtain a problem that is homogeneous in $\mathbf{u}^{(1)}$ and $p^{(1)}$, and therefore has the trivial solution $\mathbf{u}^{(1)}=\mathbf{0}$, $p^{(1)}=0$. In addition, from (31), $h^{(1)}$ (which we do *not* assume to be small as $h^{(1)}$ is a geometrical term independent of the rheology of ice) simply does not evolve at leading order. In fact, $h^{(1)}$ simply evolves slowly, at a rate that can only be determined if we include the next order in $\mu\tau_b/\eta^2$ in the problem.

We have seen that non-zero $\mathbf{u}^{(1)}$ and $p^{(1)}$ can only arise because of terms of $O(\mu\tau_b^2/\eta^2)$, and owing to the linearity of the problem, $\mathbf{u}^{(1)}$ and $p^{(1)}$ are therefore asymptotically of $O(\mu\tau_b^2/\eta^2)$ as the Reiner-Rivlin parameter $\mu\tau_b^2/\eta^2$ tends to zero. Our next step is to retain all terms that are of $O(\mu\tau_b/\eta^2)$ but omit those of higher order. This specifically requires us to retain all terms that include a factor of μ except for those that involve $u^{(1)}$, $v^{(1)}$, $w^{(1)}$ and $p^{(1)}$ multiplied by μ, since the velocity and pressure terms are themselves of $O(\mu\tau_b/\eta^2)$, and their product with $\mu\tau_b/\eta^2$ is therefore of $O(\mu^2\tau_b^2/\eta^4)$. What we are left with from (28)–(26) is then

$$\eta\left(\frac{\partial^2}{\partial y^2}+\frac{\partial^2}{\partial z^2}\right)v^{(1)}-\frac{\partial p^{(1)}}{\partial y} = 0, \quad (45)$$

$$\eta\left(\frac{\partial^2}{\partial y^2}+\frac{\partial^2}{\partial z^2}\right)w^{(1)}-\frac{\partial p^{(1)}}{\partial z} = 0, \quad (46)$$

$$\frac{\partial v^{(1)}}{\partial y}+\frac{\partial w^{(1)}}{\partial z} = 0, \quad (47)$$

combined with the boundary conditions obtained at $O(\mu\tau_b/\eta^2)$ from (31), (30) and (42):

$$w^{(1)} = -d_s\frac{\partial v^{(1)}}{\partial y}, \quad (48)$$

$$\eta\left(\frac{\partial v^{(1)}}{\partial z}+\frac{\partial w^{(1)}}{\partial y}\right)+\frac{\tau_b^2\mu}{\eta^2}\frac{\partial h^{(1)}}{\partial y} = \tau_b\frac{v^{(1)}}{u_b}. \quad (49)$$

The appearance of the factor $\tau_b^2\mu/\eta^2$ on the left-hand side of (49) is to be expected: for $h^{(1)}$ of a given size, velocity and pressure scale as the Reiner-Rivlin parameter $\mu\tau_b^2/\eta^2$ when that parameter tends to zero. Along with the far field boundary conditions

$$p^{(1)}-2\frac{\partial w^{(1)}}{\partial z}\sim 0, \qquad \frac{\partial v^{(1)}}{\partial z}+\frac{\partial w^{(1)}}{\partial y}\sim 0, \quad (50)$$

this problem fully determines $v^{(1)}$, $w^{(1)}$ and $p^{(1)}$, and decouples from the determination of the downstream velocity perturbation $u^{(1)}$.

We see that, when the Reiner-Rivlin term is small, the main coupling between bed topography and the transverse flow field appears through the basal boundary conditions: At leading order in the Reiner-Rivlin parameter $\mu\tau_b/\eta^2$, the bed perturbation $h^{(1)}$ enters into the problem for $v^{(1)}$ and $w^{(1)}$ purely through the boundary condition (49). The term responsible for the coupling is the vertical deviatoric stress term described at the end of the previous section.

3.4. Fourier transform solution and computation of growth rates for basal topography

We consider sinusoidal, time-evolving beds of the form $h(y)=\hat{h}\exp(\sigma t+iky)$ and seek solutions of the form $u^{(1)}=\hat{u}(z)\exp(\sigma t+iky)$, $p^{(1)}=\hat{p}(z)\exp(\sigma t+iky)$ etc. (or more precisely, the real parts thereof). Our aim is to find the constant σ, which determines how fast bed perturbations grow or decay.

To solve (45)–(49), we first introduce a stream function ψ such that

$$v^{(1)} = \frac{\partial \psi}{\partial z}, \qquad w^{(1)} = -\frac{\partial \psi}{\partial y}, \tag{51}$$

and (47) is satisfied automatically. The Stokes equations (45)–(46) can then be manipulated in the standard way to produce the biharmonic equation for ψ:

$$\eta \left(\frac{\partial^2}{\partial y^2} + \frac{\partial^2}{\partial z^2} \right)^2 \psi = 0, \tag{52}$$

Writing $\psi = \hat{\psi}(z) \exp(\sigma t + iky)$, the biharmonic equation becomes

$$\eta \left(\frac{\mathrm{d}^2}{\mathrm{d}z^2} - k^2 \right)^2 \hat{\psi} = 0, \tag{53}$$

with boundary conditions on $z = 0$, from (48) and (49)

$$-ik\hat{\psi} = -d_s ik \frac{\mathrm{d}\hat{\psi}}{\mathrm{d}z}, \qquad \eta \left(\frac{\mathrm{d}^2}{\mathrm{d}z^2} + k^2 \right) \hat{\psi} + ik \frac{\mu \tau_b^2}{\eta^2} \hat{h} = \frac{\tau_b}{u_b} \frac{\mathrm{d}\hat{\psi}}{\mathrm{d}z}. \tag{54}$$

and $\hat{\psi} \to 0$ as $z \to \infty$. (This far-field boundary condition is correct provided $k \neq 0$, for $k = 0$, the far-field behaviour of the stream function has to represent a constant shear.)

Solutions of (53) that satisfy the far-field conditions have the form

$$\hat{\psi} = (A + Bz) \exp(-|k|z). \tag{55}$$

The boundary conditions (54) require

$$-ikA = -d_s ik(-|k|A + B), \tag{56}$$

$$\eta(2|k|^2 A - 2|k|B) + \frac{\mu \tau_b^2}{\eta^2} ik\hat{h} = \frac{\tau_b}{u_b}(-|k|A + B). \tag{57}$$

We can therefore compute A and B:

$$\begin{aligned} A &= \frac{ik}{2\eta|k| + \tau_b/u_b} \frac{d_s \mu \tau_b^2}{\eta^2} \hat{h} \\ B &= \frac{ik(d_s|k| + 1)}{2\eta|k| + \tau_b/u_b} \frac{\mu \tau_b^2}{\eta^2} \hat{h}. \end{aligned} \tag{58}$$

Our main interest is in transverse velocities at the bed, as these can lead to transverse sediment transport and amplification of topography h, for instance through ploughing. We have

$$\begin{aligned} \hat{v}|_{z=0} &= \left. \frac{\mathrm{d}\hat{\psi}}{\mathrm{d}z} \right|_{z=0} \\ &= -|k|A + B \\ &= \frac{i\tau_b^2 \mu k}{\eta^2(2\eta|k| + \tau_b/u_b)} \hat{h}. \end{aligned} \tag{59}$$

It follows immediately that basal velocities point from trough to crest provided $\mu > 0$, which is what available data on ice indicates [*McTigue et al.*, 1985]. To see this more clearly, suppose that h is a cosine wave, so $\hat{h}$ is real and positive. Then $v|_{z=0}$ is a negative sine wave in y, i.e. the velocity to the right of the crest at $y = 0$ points in the negative y-direction, and therefore towards the crest. A contour plot of Ψ for a bed in the shape of a cosine wave is also included in figure 2.

We therefore see that, provided $\mu > 0$, the rheological nonlinearity of a Reiner-Rivlin rheology for ice fashions a plausible mechanism for amplification of basal flutes: the transverse basal velocities calculated here are liable to transport basal sediment from troughs in the bed towards ridges in the bed, thus amplifying topography. We can confirm this by computing the growth coefficient σ from (31):

$$\sigma = \frac{d_s \tau_b^2 \mu k^2}{\eta^2(2\eta|k| + \tau_b/u_b)}. \tag{60}$$

Hence we find the exponentially growing solutions

$$h = \hat{h} \exp\left[\frac{d_s \tau_b^2 \mu k^2}{\eta^2(2\eta|k| + \tau_b/u_b)} t + iky \right], \tag{61}$$

with the expected feature that h grows over time provided $\mu > 0$. There is, however, a problem. As $k \to \infty$, the growth rate increases linearly in k, and short wavelengths are violently unstable. The evolution problem is not well-posed. The simplest remedy is to suppose that, in addition to a ploughing flux, there is gravitationally driven sediment slumpage down bed gradients. In that case, the flux prescription in (12) can be amended to include an additional term

$$\mathbf{q}_s = d_s \left[u\mathbf{i} + v\mathbf{j} \right]|_{z=0} - \alpha \frac{\partial h}{\partial y} \mathbf{j}, \tag{62}$$

so that sediment partly flows down gradients in h. Repeating the calculation leading up to (61), we find a growth rate of the form

$$\sigma = \frac{d_s \tau_b^2 \mu k^2}{\eta^2(2\eta|k| + \tau_b/u_b)} - \alpha k^2,$$

which is negative for large k, corresponding to stable short wavelengths. There is then also a preferred, fastest growing wavelength determined by the interplay between rheology-driven topography amplification and gravitationally driven sediment diffusion. This wavelength however depends sensitively on the diffusion coefficient α, which cannot be constrained accurately here. In fact, what this result really points to is the need for a better model for sediment transport by the ice, an issue that needs to be taken up by further work.

Nonetheless, we can make a number of observations about growth rates. We discuss these in the next section.

4. Discussion

The stability analysis has shown that, if $\mu > 0$, transverse basal flows will be directed from the troughs in a sinusoidally fluted bed to the crests of the bed, causing amplification of the flutes at least when they are small and the flow problem can be linearized. In order to estimate growth rates for the formation of subglacial bedforms on the basis of our theory, we require estimates for the rheological parameters involved. The main constraint here is the absence of reliable data covering the temperature and stress regimes that are pertinent to basal ice. Existing data sets on normal stress effects are those due to *McTigue et al.* [1985] and *Man and Sun* [1987].

On the basis of biaxial creep tests conducted on polycrystalline ice at axial deviatoric stresses of 0.47 MPa (which exceeds typical glacial driving stresses by a factor of around 5) and at temperatures of around -9.5° C, *McTigue et al.* [1985] estimate the viscosity parameter μ as lying in a range between 2.5×10^{21} to 5.9×10^{22} Pa s^2, with a mean between all experiments of 3.4×10^{21} Pa s^2. Importantly for the instability mechanism, we invariably have $\mu > 0$. Conversely, the ordinary viscosity η estimated by these authors has a mean

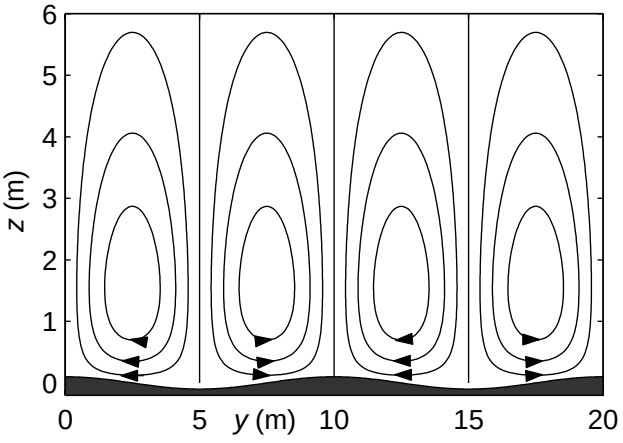

Figure 2. Illustration of transverse spiral flow, vertically exaggerated. The main ice flow direction is into the page. The wavelength of the cosine-shaped bed topography shown as a grey patch at the bottom is 10 m, and amplitude is 10 cm. Shown are contours of the stream function (i.e., streamlines), with the direction of flow indicated by arrows. Contour intervals for $\Psi/(\mu\tau_b/\mu^2)$ (i.e., stream function scaled with the Reiner-Rivlin parameter $\mu\tau_b/\mu^2$, which is introduced here to remove the dependence on the poorly constrained parameter μ) are 10^{-9} m^2 s^{-1} = 0.0315 m^2 a^{-1}. Parameters are $d_s = 5 \times 10^{-2}$ m, $\tau_b = 10^5$ Pa, $u_b = 10$ m a^{-1} $= 3 \times 10^{-7}$ m s^{-1} and $\eta = 8 \times 10^{12}$ Pa s. The important feature here is that velocities at the bed are directed *towards* the flute crests.

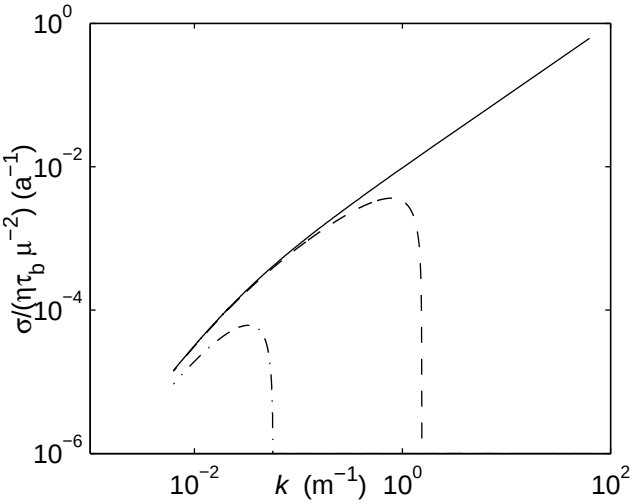

Figure 3. Logscale plot of growth rate (scaled with the Reiner-Rivlin parameter $\eta\tau_b/\mu^2$) against wavenumber (the scaling is performed in order to remove the dependence on the poorly constrained parameter μ). Parameters are $d_s = 5 \times 10^{-2}$ m, $\tau_b = 10^5$ Pa, $u_b = 10$ m a^{-1} $= 3 \times 10^{-7}$ m s^{-1} and $\eta = 8 \times 10^{12}$ Pa s. Shown are the ill-posed case in which there is no sediment slumpage ($\alpha = 0$) as a solid line, as well as the cases $\alpha = 0.076$ m^2 a^{-1} (dashed) and $\alpha = 0.127$ m^2 a^{-1} (dot-dashed), for which a fastest growing wavenumber can be identified, which clearly depends sensitively on α. In the former case, the fastest growing wavelength is around 6 m, in the latter around 150 m.

value of 4.5×10^{15} Pa s, so in their regime, $\mu\tau_b/\eta^2 = 0.78$ with τ_b =0.47 MPa. Clearly, deviatoric normal stresses associated with the second term in the Reiner-Rivlin rheological equation (1) are of nearly the same magnitude as those associated with the first term describing ordinary viscosity, pointing to the possibility that normal stress effects could play an important role in realistic glacier flow settings.

That said, the rheology of ice is significantly non-linear, and the results computed by *McTigue et al.* [1985] are, by their own admission, quantitatively not very well constrained. It is therefore unclear what an appropriate value for μ would be for more typical deviatoric stresses of around 0.1 MPa, and for the temperate ice typically found in the basal layers of a glacier or ice sheet that is sliding over its bed. To make progress, we assume that the ratio $\mu\tau_b/\eta^2$ that remains smaller than unity (so our theory applies) but is not extremely small, so that we can estimate growth rates based on equations (61) or (62).

We take $d_s = 5$ cm as a till deformation depth scale, while we put $\tau_b = 10^5$ Pa, $u_b = 10$ m a^{-1} $= 3 \times 10^{-7}$ m s^{-1}, and estimate η from Glen's law with A and n denoting the usual parameters *Paterson* [1994, chapter 5]. With $\eta \sim 1/(2A\tau^{n-1})$ and $n = 3$, $A = 6 \times 10^{-24}$ Pa^{-3} s^{-1}, we have $\eta = 8 \times 10^{12}$ Pa s. These values form the basis of the growth rate (figure 3) and the velocity field plot (figure 2).

The growth rates obtained here are relatively small: for a one-metre wide flute ($k = 2\pi$ m^{-1}) and $\eta\tau_b/\mu^2 = 0.5$, the growth rate (inverse e-folding time) of roughness amplification (in the absence of gravity-driven sediment slumpage, so $\alpha = 0$) is roughly 0.03 a^{-1}, while for a much larger, 300-metre wide flute ($k = 2\pi/300$ m^{-1}), it is 5×10^{-5} a^{-1}. The first of these may be attainable for valley glaciers (flute growth would take a few decades, which is compatible with the estimates in *Rose* [1989], but is slower than the annual time scale for very small flutes observed by *van der Meer* [1997]), while the second undoubtedly is too small to produce the mega-scale lineations observed as having formed under ice sheets. However, the growth rate computed in (61) scales directly with d_s, and a deeper rate of ploughing depth will give a higher till flux, and consequently a faster-growing subglacial bedform. For instance, increasing depth scale d_s for sediment movement from 5 cm to 1 m [roughly the thickness of till mantles on drumlins observed in e.g. *Alden*, 1905] decreases the formation timescale for a 300 m wide megalineation to a more realistic 10^{-3} a^{-1}, meaning that the growth of a lineation takes about 1000 years. At this point, it can be questioned whether ploughing by itself would be sufficient to provide the necessary depth of sediment deformation, and it is possible that distributed shear in the sediment as described by *Boulton and Hindmarsh* [1987] and *Tulaczyk et al.* [2000] may be required. Similarly, growth rates computed in (61) and (62) increase with decreasing ice viscosity η, and with increasing basal sliding velocity u_b, as both of these make the denominator smaller. It transpires that realistic growth rates may still be possible, but settling the issue will require further research into subglacial sediment transport. An interesting point here is also that flute-type topography may form very rapidly: there are no direct observations of flute-formation, but *Smith et al.* [2007] observed the formation of an elongated feature with a height of over ten metres at the bed Rutford ice stream, inferred to be composed of sediment, over the space of a few years. Based on the estimates above, it appears unlikely that our theory can account for such rapid bedform formation, given the values of μ inferred by *McTigue et al.* [1985]. Faster growth rates may be obtained for larger values of μ, but these should also lead to normal stress effects becoming more noticeable in general ice flow situations (such as the surface depression

at glacier centrelines computed by *McTigue et al.* [1985]), and therefore appear to be unfeasible unfeasible.

As we indicated in the introduction, smaller flutes under valley glaciers and megaflutes may be formed by different processes, as seems plausible due to the large disparity in physical scales. A widely accepted hypothesis for the formation of small-scale flutes which does not apply to megaflutes is due to *Boulton* [1976], who notes the frequent occurrence of boulders at the upstream end of flutes and regards these as a necessary ingredient in the formation of small-scale flutes. Essentially, Boulton's theory states that a cavity opens between ice and bed in the lee of the boulder [in the manner envisaged by *Lliboutry*, 1968], and this cavity is then filled by till being extruded into it.

However, even for the typically low effective pressures found at the beds of glaciers, it is difficult to conceive of such long cavities extending in the rear of a relatively small bed protuberance, and moreover, one would expect their height to attenuate noticably in the lee of the protuberance. Interestingly, Boulton notes such an attenuation only in the immediate lee of the boulder, but not further downstream. A possible alternative interpretation of Boulton's paper (especially in view of figure 8d therein, which indicates a cavity propagating downstream) is that he envisages the lee-side cavity filling with till, with this till ridge then somehow generating a further cavity in its lee, which can then be filled and so forth. This image is however also fraught with conceptual difficulty: to begin with, the till must be sufficiently soft to be extruded into the cavity, but subsequently it must turn immobile to act as an essentially rigid body that supports a cavity in its lee. More crucially still, this process also requires that the extruded till pushes the ice roof of the cavity upwards: if this did not happen, then the extruded till would simply fill the lee-side cavity behind the boulder until it is in contact with the ice, and there would be no mechanism for the cavity to extend further. Only if the extruded till pushes up on the ice roof (and thus acts as an obstacle that was previously not present and that ice now has to flow over or around) can the cavity be extended. To put this in a different way, if one were to take the cavities in the theoretical computations of *Fowler* [1986], *Schoof* [2005] and *Gagliardini et al.* [2007] and fill them with bedrock, the lower boundary in the ice would still remain in the same place; only if bedrock was pushed up into the ice could additional cavities form. However, as till is denser than ice, it is difficult to see why the extruded till should push the overlying ice upwards and extend the lee-side cavity in this manner unless.

Consequently, Boulton's hypothesis may represent an incomplete picture of small-scale flute formation, and further modelling is required to validate it. Our model furnishes a possible alternative to Boulton's mechanism, one which does not require a protuberance but which is not in conflict with the observation that many flutes start at boulders, as these will naturally act as seeds for an instability mechanism. Observing the frequent occurrence of flutes that do not initiate at a boulder, *Rose* [1989] alludes to transverse 'flow cells' in basal ice that could explain the formation of flutes, and speculates that boulders could be natural starting points for such flow cells without being necessary for their We suggest that our theory indicates a possible origin of precisely such flow cells. Transverse flow cells of this kind are also compatible with the general observation of till fabrics indicating the flow of till from inter-flute trough towards the flute crest noted by *Shaw and Freschauf* [1973] for megaflutes and by *Boulton* [1976] for smaller flutes and reproduced by other researchers since [*Benn*, 1994; *Rose*, 1989], though not universally [*Eklund and Hart*, 1996; *Hubbard and Reid*, 2006]. The absence of a herringbone-type pattern could, of course simply indicate a weak transverse flow component.

At a larger scale, the groove-ploughing hypothesis of *Clark et al.* [2003] is somewhat similar to Boulton's flute-formation theory in that it assumes an association between megaflute and an upstream obstruction; by contrast with Boulton's theory, Clark et al. do not assume that elongated cavities form behind these obstructions but rather that ice keels remove sediment from the ice sheet bed in a manner similar to a rake, leaving behind the ridges that are identified as megaflutes. As with Boulton's theory, there is again evidence that megaflutes need not correspond directly to an initiating bed protuberance upstream [e.g. *Ó Cofaigh et al.*, 2005], and our theory provides an alternative explanation that does not conflict with upstream obstacles but neither conflicts with their presence.

Lastly, it is worth pointing out that our theory does not fit neatly into the debate over erosional or depositional origins for subglacial bedforms [e.g. *Hart*, 1997], but is essentially a till-deformation based theory. That said, the distinction between these is possibly artificial: according to our theory, sediment is removed from the troughs between flutes and deposited at the crests, so it comprises elements of both, erosion and deposition. Moreover, if there is net sediment removal or deposition (for instance through freeze-on or melt-out) acting in parallel with the lateral transport of sediment envisaged by our theory, the flute that is observed after the fact may appear to be erosional or depositional in nature, but this will not indicate the process involved in the formation of the flute pattern, as this requires selective erosion or deposition.

As pointed out in the introduction, our intention in this paper was mostly conceptual, and as such, the relative merits of our theory versus competing ones such as those of *Boulton* [1976] or *Clark et al.* [2003] cannot be properly assessed. It is possible that ours may be more appropriate to larger-scale bedforms such as megaflutes while a version of Boulton's captures the formation of small-scale flutes, or that there is more than one formation mechanism at work. Only a fully nonlinear model coupled with a more sophisticated description of till flow than that used here would be required allow detailed comparisons to be made with field observations of exposed flutes. A tantalizing alternative to such observations would, of course, be the direct study of potential secondary flows in basal ice.

5. Conclusions

In this paper, we have considered the effect of so-called normal stress effects in a general viscous rheology for ice on the flow of ice near the bed and its implications for the formation of subglacial topography.

Experimental evidence [*McTigue et al.*, 1985; *Man and Sun*, 1987] has shown that the deviatoric stress generated by a given strain rate in ice is not in general parallel to the strain rate tensor. In particular, a simple shearing flow will generate normal stresses perpendicular to the flow direction. This behaviour can be captured by a Reiner-Rivlin rheology as formulated in equation (1) in this paper.

A consequence of these normal stresses is that additional stresses can be required to balance them, and that these stresses can somtimes only be genereated secondary, transverse flows. This happens when the normal stresses in the basic shearing flow are not uniform, as will be the case when there is bed topography at the base of the ice. In this paper, we have studied how ridges in the bed aligned with the main ice flow direction can cause such secondary, transverse flows. We have found that, for the parameter regimes indicated by the available experimental evidence, the transverse flows are such that velocity at the bed is directed from the troughs of basal ridges to their crests (figure 3). If there is a basal sediment flux associated with the movement of ice over the bed, then a transverse movement of ice from the troughs of

bed ridges to their crests, as indicated in figure 3, will cause the amplification of basal ridges. In essence, this is the formation mechanism for subglacial lineations hypothesized by *Shaw and Freschauf* [1973].

While this mechanism has been shown to be plausible, several issues remain outstanding. Firstly, the growth rates predicted by the theory are relatively small, and consequently may not suffice to generate the large-scale flutings formed by the major mid-latitude ice sheets of the last ice age. A crucial component here is the description of subglacial sediment transport by the overriding ice: the growth rate scales with the depth to which subglacial sediment is deformed. In order to produce bedforms rapidly, larger sediment fluxes are required, and these in turn imply a greater depth to which sediment must be deformed. In order to resolve this issue, additional work in the area of subglacial sediment transport by overriding ice is required.

A second issue that is unresolved is the selection of a preferred wavelength that is amplified. The basic model in this paper predicts that shorter wavelength invariably grow faster than long wavelengths, and that growth rates become unbounded at short wavelengths. This is clearly the result of the particular parameterization of subglacial sediment transport chosen in the model, which assumes that sediment flux is simply proportional to basal ice velocity. This parameterization lacks a mechanism for stabilization at short wavelengths, which may for instance arise if sediment flux is driven partly by a downslope component of gravity as outline in section 3.4. However, the sediment transport component of the theory was not the main focus of this work, and we defer further consideration to future research. In addition, there are other rheological models from (1) that capture normal stress effects, notably the 2nd grade rheology also considered by *Man and Sun* [1987] (which additionally has the advantage over the model considered here that the Clausius-Duhem inequality can be satisfied with constant model coefficients, see the note below), and these rheological models could also produce different bedform amplification from the model studied here.

6. Acknowledgements

This work was supported by the U.S. National Science Foundation through grant number DMS-03227943. Many thanks to Joe Walder and Martin Lüthi for pointing us towards McTigue *et al.*'s (1987) paper, and to Martin Truffer and Richard Hindmarsh for their thorough reviews. GKCC wishes to acknowledge inspiring discussions with John Shaw, more than two decades ago, that provided the seed for this work.

Notes

1. Strictly speaking, μ cannot be a constant for all strain rate tensors $\mathbf{D}$ if the Clausius-Duhem inequality is to be satisfied [*Eringen*, 1962], but must depend on the second and third invariants of $\mathbf{D}$. This is the case because the rate of shear heating is given by $\tau_{ij}D_{ij} = 2\eta D_{ij}D_{ij} + 4\mu D_{ik}D_{kj}D_{ij}$. The first of these two terms is proportional to the second invariant of $\mathbf{D}$, i.e., a sum of squares and therefore intrinsically non-negative. The second term on the other hand is proportional to the third invariant of $\mathbf{D}$, and can change sign. However, negative shear heating is not an issue provided the second term in the shear heating expression is small, and our linearization scheme will assume precisely that. Hence the assumption of constant μ remains self-consistent in our linearization scheme.

References

Aario, R. (1977), Flutings, drumlins and rogen-landforms, *Nordia*, *2*, 5–14.

Alden, W.C. (1905), The drumlins of southeastern Wisconsin, *U.S. Geol. Surv. Bull. ser. B*, *76*, 9–46.

Benn, D.I. (1994), Fluted moraine formation and till genesis below a temperate valley glacier: Slettmarkbreen, Jotunheimen, Southern Norway, *Sedimentology*, *41*, 279–292.

Boulton, G.S. (1976), The origin of glacially fluted surfaces — observations and theory, *J. Glaciol.*, *17*(76), 287–309.

Boulton, G.S. (1987), A theory of drumlin formation by subglacial sediment deformation, in *Drumlin Symposium*, edited by J. Menzies and J. Rose, pp. 25–80, Balkema, Rotterdam.

Boulton, G.S., and R.C.A. Hindmarsh (1987), Sediment deformation beneath glaciers: rheology and geological consequences, *J. Geophys. Res.*, *92*(B9), 9059–9082.

Clark, C.D., S.M. Tulaczyk, C.R. Stokes, and M. Canals (2003), A groove-ploughing theory for the production of mega-scale glacial lineations, and implications for ice-stream mechanics, *J. Glaciol.*, *49*(165), 240–256.

Dowdeswell, J.A., C. Ó Cofaigh, and C.J. Pudsey (2004), Thickness and extent of the subglacial till layer beneath and antarctic paleo-ice stream, *Geology*, *32*(1), 13–16, doi:10.1130/GI19,864.1.

Eklund, A., and J.K. Hart (1996), Glaciotectonic deformation within a flute from Isfallsglaciären, Sweden, *Journal of Quaternary Science*, *11*(4), 299–310.

Eringen, A.C. (1962), *Nonlinear theory of continuous media*, McGraw-Hill, New York.

Fowler, A.C. (1981), A theoretical treatment of the sliding of glaciers in the absence of cavitation, *Phil. Trans. R. Soc. Lond.*, *298*(1445), 637–685.

Fowler, A.C. (1986), A sliding law for glaciers of constant viscosity in the presence of subglacial cavitation, *Proc. R. Soc. Lond. A*, *407*, 147–170.

Fowler, A.C. (2000), An instability mechanism for drumlin formation, in *Deformation of glacial materials*, *Spec. Pub. Geol. Soc.*, vol. 176, edited by A. Maltman, M.J. Hambrey, and B. Hubbard, pp. 307–319, The Geological Society, London.

Fowler, A.C. (2001), Modelling the flow of glaciers and ice sheets, in *Continuum Mechanics and Applications in Geophysics and the Environment*, edited by B. Straughan, R. Greve, H. Ehrentraut, and Y. Wang, pp. 276–304, Springer-Verlag, Berlin.

Gagliardini, O., D. Cohen, P. Raback, and T. Zwinger (2007), Finite-element modeling of subglacial cavities and related friction law, *J. Geophys. Res.*, *112*(F2), F02,027, doi:10.1029/2006JF000,576.

Glen, J.W. (1958), The flow law of ice. a discussion of the assumptions made in glacier theory, their experimental foundation and consequences, in *Physics of the Movement of Ice — Symposium at Chamonix 1958*, pp. 171–183, IASH.

Glückert, G. (1973), Two large drumlin fields in central finland, *Fennia*, *120*, 5–37.

Gravenor, C.P. (1953), The origin of drumlins, *Am. J. Science*, *251*, 674–687.

Hart, J.K. (1997), The realtionship between drumlins and other forms of subglacial glaciotectonic deformation, *Quat. Sci. Rev.*, *6*, 93–107.

Hindmarsh, R.C.A. (1998), The stability of a viscous till sheet coupled with ice flow, considered at wavelengths less than the ice thickness, *J. Glaciol.*, *44*(146), 285–292.

Hubbard, T.D., and J.R. Reid (2006), Analysis of flute forming conditions using ice sheet reconstructions and field techniques, *Geomorphology*, *74*, 137–151.

Iverson, N.R., T.S. Hooyer, and R.W. Baker (1998), Ring-shear studies of till deformation: Coulomb-plastic behaviour and distributed shear in glacier beds, *J.Glaciol.*, *44*(148), 634–642.

Lliboutry, L. (1968), General theory of subglacial cavitation and sliding of temperate glaciers, *J. Glaciol.*, *7*(49), 21–58.

Lundqvist, J. (1969), Problems of the so-called rogen-moraine, *Sveriges Geologiska Undersökning Ser. C Årsbok*, *64*(5), 3–32.

Man, C.S., and Q.X. Sun (1987), On the significance of normal stress effects in the flow of glaciers, *J. Glaciol.*, *33*(115), 268–273.

McTigue, D.F., S.L. Passman, and S.J. Jones (1985), Normal stress effects in the creep of ice, *J. Glaciol.*, *31*(108), 120–126.

Menzies, J., and J. Rose (Eds.) (1987), *Drumlin Symposium*, Balkema, Rotterdam.

Morris, E.M., and L.W. Morland (1976), A theoretical analysis of the formation of glacial flutes, *J. Glaciol.*, *17*(76), 311–323.

Mosola, A.B., and J.B. Anderson (2006), Expansion and rapid retreat of the West Antarctic Ice Sheet in eastern Ross Sea: possible consequence of over-extended ice streams, *Quat. Sci. Rev.*, *25*, 2177–2196.

Nye, J.F. (1965), The flow of a glacier in a channel of rectangular, elliptic or parabolic cross-section, *J. Glaciol.*, *5*(41), 661–690.

Ó Cofaigh, C., J.A. Dowdeswell, C.S. Allen, J.F. Hiemstra, C.J. Pudsey, J. Evans, and D.J.A. Evans (2005), Flow dynamics and till genesis associated with a marine-based antarctic palaeo-ice stream, *Quat. Sci. Rev.*, *24*, 709–740.

Ottesen, D., and J.A. Dowdeswell (2006), Assemblages of submarine landforms produced by tidewater glaciers in svalbard, *J. Geophys. Res.*, *111*(F01016), doi:10.1029/2005JF000,330.

Parrenin, F., and R.C.A. Hindmarsh (2007), Influence of a non-uniform velocity field on isochrone geometry along a steady flowline of an ice sheet, *J. Glaciol.*, *53*(183), 612–622.

Paterson, W.S.B. (1994), *The Physics of Glaciers*, 3rd ed., Pergamon, Oxford.

Reynaud, L. (1973), Flow of a valley glacier with a solid friction law, *J. Glaciol.*, *12*(65), 251–258.

Rose, J. (1989), Glacier stress patterns and sediment transfer associated with the formation of superimposed flutes, *Sedimentary Geology*, *62*, 151–176.

Schoof, C. (2002), Basal perturbations under ice streams: form drag and surface expression, *J.Glaciol.*, *48*(162), 407–416.

Schoof, C. (2004), On the mechanics of ice stream shear margins, *J. Glaciol.*, *50*(169), 208–218.

Schoof, C. (2005), The effect of cavitation on glacier sliding, *Proc. R. Soc. Lond. A*, *461*, 609–627, doi:10.1098/rspa.2004.1350.

Schoof, C. (2006a), Variational methods for glacier flow over plastic till, *J. Fluid Mech.*, *555*, 299–320.

Schoof, C. (2006b), A variational approach to ice-stream flow, *J. Fluid Mech.*, *556*, 227–251.

Schoof, C. (2007a), Pressure-dependent viscosity and interfacial instability in coupled ice-sediment flow, *J. Fluid Mech.*, *570*, 227–252.

Schoof, C. (2007b), Cavitation on deformable glacier beds, *SIAM J. Appl. Math.*, *67*(6), 1633–1653.

Shaw, J. (1983), Drumlin formation related to inverted meltwater erosion marks, *J. Glaciol*, *29*(103), 461–479.

Shaw, J., and R.C. Freschauf (1973), A kinematic discussion of the formation of glacial flutings, *Canadian Geographer*, *18*, 19–35.

Smalley, I.J., and D.J. Unwin (1968), The formation and shape of drumlins and their distribution and orientation in drumlin fields, *J. Glaciol.*, *7*(51), 377–390.

Smith, A., T. Murray, K. Nicholls, K. Makinson, and G. Adalgeirsdottir (2007), Rapid erosion, drumlin formation, and changing hydrology beneath an antarctic ice stream, *Geology*, *35*(2), 127–130.

Smith, H.T.U. (1948), Giant glacial grooves in northwest canada, *Am. J. Sci.*, *246*, 503–514.

Tarr, R.S. (1894), The origin of drumlins, *Am. Geologist*, *13*, 393–407.

Truffer, M., and K.A. Echelmeyer (2003), Of isbrae and ice streams, *Ann. Glaciol.*, *36*, 66–72.

Tulaczyk, S., W.B. Kamb, and H.F. Engelhardt (2000), Basal mechanisms of ice stream b, west antarctica: 1. till mechanics, *J. Geophys. Res.*, *105*(B1), 463–481.

van der Meer, J.J.M. (1997), Short-lived streamlined bedforms (annual small flutes) formed under clean ice, Turtmann Glacier, Switzerland, *Sedimentary Geology*, *111*, 107–118.

van der Veen, C.J., and I.M. Whillans (1990), Flow law for glacier ice: comparisons of numerical predictions and field measurements, *J. Glaciol.*, *36*(124), 324–339.

Weertman, J. (1957), On the sliding of glaciers, *J. Glaciol.*, *3*(21), 33–38.

Christian G. Schoof and Garry K.C. Clarke, Department of Earth and Ocean Sciences, University of British Columbia, 6339 Stores Road, Vancouver, V6T 1Z4, Canada. (cschoof@eos.ubc.ca)